Journal of Environmental Chemical Engineering 10 (2022) 108617

Contents lists available at ScienceDirect

Journal of Environmental Chemical Engineering

journal homepage: www.elsevier.com/locate/jece

Exploring the effect of the pulp bleaching on the thermo-rheological behavior of sustainable cellulose nanofiber-based oleogels

Claudia Roman [1], Miguel A. Delgado [2,*], Samuel D. Fernández-Silva [3], Moisés García-Morales [4]

Departamento de Ingeniería Química, Centro de Investigación en Tecnología de Productos y Procesos Químicos (Pro2TecS), Campus de "El Carmen", Universidad de Huelva, 21007 Huelva, Spain

ARTICLE INFO

Editor: Xiwang Zhang

Keywords:
Cellulose nanofibers
Bleaching
Castor oil
Sustainability
Rheology
Lubricants

ABSTRACT

Taking advantage of the high thickening capacity of cellulose nanofibers in castor oil, sustainable lubricating oleogels were obtained. Methanol was used as mediator to transfer the nanofibers, originally present as a hydrogel, into the vegetable oil. The effect of the pulp bleaching on the oleogels' thermo-rheological behavior was analyzed. Viscous flow curves and small/large amplitude dynamic shear tests were carried out on both bleached and unbleached samples of the same elm kraft pulp. Substantial differences were observed, above all when the oleogels were subjected to stress values beyond the onset of their linear viscoelastic regimes. The oleogel prepared with nanofibers from the unbleached pulp was found to endure large shear deformations better than that from the bleached pulp, and was less sensitive to temperature. Hence, the complex shear modulus (|G*|) corresponding to the oleogel based on 1.4 wt% bleached nanofiber decreased by 55.7% upon a non-linear stress of 200 Pa was applied for 30 min. However, a less severe structural breakdown, i.e., a decay in |G* | of 28.9% (half of the previous one), was monitored when the oleogel based on the unbleached nanofiber was submitted to the same testing conditions. It should also be underlined that such an oleogel showed an extraordinary capacity to recovery its structure after the large shear deformation process.

1. Introduction

Lubricating greases play a vital role when a reduction in friction and wear is needed but lubricating oils, not sufficiently viscous, are not suited options. Most of them are constituted by mineral oils and a non-biodegradable thickener. Hence, the global greater use of lubricants and their uncontrolled disposal into the environment upon their use have motivated the replacement of the petroleum-derived feedstocks with more sustainable and non-toxic products [1]. It is important to remark that ecolubricants are being lately demanded by industries which develop the production of fully sustainable of energy with zero emissions, e.g., the field of wind turbine blade bearings applications, where they are in direct contact with the environment.

A way of producing eco-friendly lubricating greases is the replacement of the main component, i.e., the base oil, with renewable and biodegradable sources such as vegetable oils [2]. Vegetable oils are universally available, non-toxic and often an inexpensive choice. Attempts of substituting mineral and synthetic oils with vegetable oils can be found elsewhere, as reviewed by Panchal et al. [2] and Narayana Sarma and Vinu [3]. Among them, it is worth highlighting that Quinchia et al. [4] demonstrated a suitable tribological behavior of vegetable oil-based lubricants. Due to its high viscosity and good thermal stability, castor oil has become the most used. These authors also found a cellulose derivative, i.e. the ethyl cellulose, which acts as multifunctional additive for blends of vegetable oil-based lubricants, demonstrating a better compatibility with castor oil than with high oleic sunflower oil [5]. It is also noteworthy that used cooking oils can be exploited as second-generation raw materials for the synthesis of green formulations. In this sense, Fernández-Silva et al. [6] analyzed the potential valorization of waste cooking oils into sustainable bio-lubricants, which is

* Corresponding author.
E-mail addresses: claudia.roman@diq.uhu.es (C. Roman), miguel.delgado@diq.uhu.es (M.A. Delgado), samuel.fernandez@diq.uhu.es (S.D. Fernández-Silva), moises.garcia@diq.uhu.es (M. García-Morales).
[1] ORCID: 0000–0002-7960–5832
[2] ORCID: 0000–0003-0573–7987
[3] ORCID: 0000–0001-6253–1497
[4] ORCID: 0000–0003-4153–487X

https://doi.org/10.1016/j.jece.2022.108617
Received 11 July 2022; Received in revised form 6 September 2022; Accepted 16 September 2022
Available online 17 September 2022

very relevant from a circular economy standpoint. Moreover, the development of fully biodegradable lubricating greases requires the identification of proper eco-substitutes for the traditional thickening agents (such as lithium, aluminum, sodium and calcium soaps, polyureas, etc.). In this way, previous studies have demonstrated that biopolymers from natural sources, mainly lignocellulosic materials, may act as thickening agents which, in vegetable oil, yield semi-solid formulations with appropriate rheological and tribological properties [7,8].

Over the last decades, cellulose nanomaterials have gained increasing acceptance as reinforcing and thickening agents even at very low concentration and with no need for further chemical modification. Cellulose nanomaterials are characterized by their non-toxicity, renewability, bio-degradability, high surface area, high aspect ratio, light weight, adaptable surface chemistry, and exceptional mechanical and optical properties [9]. Even so, their prospects of being used in fully sustainable lubricating formulations depend on their correct dispersion in vegetable oil. Upon nanofibrillation, nanocellulose materials are commonly available as hydrogels with a solid content between 1 and 15 wt% [10,11]. Their complete dehydration would cause irreversible hornification, which would hinder their further re-dispersion [12]. The biggest challenge is, thus, to find new strategies that enable their direct migration from water into oily phase [13]. In this context, a methanol-based solvent exchange method enabling the production of homogenous and stable cellulose nanofibrils oleogels has been recently published by the authors [14]. Methanol was shown to successfully assist the transfer of elm wood cellulose nanofibrils from the starting hydrogel to castor oil without affecting their dispersibility and their thickening capacity.

Regarding the cellulose nanofibrils isolation process, the chemical pulp fibers are submitted to high-shear mechanical treatment by high-pressure homogenizers or microfluidizers which fibrillates them into high aspect ratio nanofibers [15–17]. According with Iglesias et al. [18], there is significant controversy regarding whether or not the presence of lignin aids the mechanical separation of the individual fibrils in the plant cell wall. In this work, both bleached and unbleached chemical pulps were used as starting materials for CNFs production by PFI mills [17]. On the one hand, unbleached pulps lead to non-oxidized cellulose nanofibers with high lignin and hemicelluloses content, and offer the advantage of reduced processing costs and environmental impact [18]. On the other hand, totally bleached chemical pulps result in cellulose nanofibers with only trace amounts of residual lignin and hemicelluloses and a higher crystallinity [19]. Even though bleached and unbleached chemical pulps yield different nanofibers in terms of their surface chemistry and aspect ratio [18,19], to the best of our knowledge no much studies have been yet conducted on the incorporation of CNFs in vegetable oils and their effect on the thermo-rheological behavior of theirs oleogels. Hence, we hypothesize that “cellulose nanofibers from bleached and unbleached chemical pulps may yield oleogels with noticeably different thermo-rheological behaviors”.

In terms of performance, particular applications may require a lubricating grease which performs efficiently under changing operating conditions involving a wide temperature range. Severe temperature variations may produce significant physical and/or chemical changes, which frequently contribute to a premature failure of the lubrication phenomena. Moreover, as Delgado et al. [20] pointed out, it results fundamental to find out how the lubricating grease is affected by large amplitude deformations, as well as to assess their capacity to recover their initial state after such a deformation beyond the LVE threshold ceases.

Based on all above ideas, the goal of this research work was to investigate the effect, if any, of the pulp bleaching process on the thermo-rheological behavior of sustainable oleogels based on elm wood cellulose nanofibers and castor oil. We report a thermo-rheological characterization, up to 180 ºC, based on viscous flow curves and small/large amplitude dynamic shear tests which confirmed the above stated hypothesis.

2. Materials and methods

2.1. Raw materials

Castor oil, with kinematic viscosity at 40 ºC of 242.5 cSt, supplied by Guinama (Spain) was selected as vegetable base oil. Basic properties and compositional details of castor oil can be found elsewhere [21].

Two different types of cellulose nanofibers from elm wood pulp, produced by PFI refining prior to microfluidization, were provided by Forest Research Centre, INIA-CSIC, Madrid (Spain). One type of nanofiber comes from an elm kraft pulp which was subjected to bleaching (CNF-B) whereas in the second type of nanofiber the elm kraft pulp was used as such (CNF-U). Cellulose nanofibers production and characterization followed the protocols described in Jiménez-López et al. [22].

2.2. Oleogels preparation

Cellulose nanofibers were supplied as gel-like aqueous suspensions having solid contents of ca. 2 wt%. CNFs incorporation into castor oil involved a solvent exchange method using methanol, as previously reported in Roman et al. [14]. Homogeneous and storage-stable oleogels with nanofiber contents of 0.7 and 1.4 wt% were obtained and studied. These oleogels showed high penetration values, i.e., low NLGI grade between 00 and 000 (according to one-quarter-scale penetration values, in ASTM D217). For the sake of looking further into the effect of concentration, an extra formulation with 2.8 wt% CNF-B was also analyzed. Such an oleogel achieved a higher NLGI grade, between 1 and 2.

2.3. Oleogels characterization

Three types of rheological tests were carried out in a controlled-stress rheometer Physica MCR-301 (Anton Paar, Austria) equipped with a rough plate-and-plate geometry (25 mm diameter and 1 mm gap). The oleogels’ linear viscoelastic behavior was evaluated through isothermal dynamic shear frequency sweeps at stress values within the linear viscoelastic (LVE) range, in a frequency interval from 0.08 to 100 rad/s. Such tests were carried out at selected temperatures between 25 and 180 ºC. The LVE range was previously identified by performing dynamic stress sweep tests at a fixed frequency of 6.28 rad/s (1 Hz), at the lowest and the highest temperatures, 25 and 180 ºC, respectively. The LVE was characterized by a stress critical value below which the viscoelastic functions remain stress-independent. Moreover, viscous flow curves were performed in a shear rate range between 10^{-2} and 10^{2} s^{-1}, also at selected temperatures between 25 and 180 ºC.

In order to evaluate the greases’ mechanical stability under large amplitude oscillatory shear (LAOS) conditions, they were subjected to the following protocol, similar to that reported by Delgado et al. [20], consisting in three consecutive dynamic shear time sweeps, at 6.28 rad/s (1 Hz) and 25 ºC: a) an initial 5 min interval of loading under a stress within the LVE regime, which provided the complex modulus value associated to the unaltered state of the sample, $|G_0^*|$; b) an intermediate 30 min interval under a stress outside the LVE regime, which led to structural damage in the sample, $|G_1^*|$; c) a final 30 min interval under the same stress applied in step a), over which the initial state is partially recovered, $|G_2^*|$. Two non-linear stress values of 100 and 200 Pa were selected. A third stress value of 20 Pa, at the limit of the LVE regime, was also studied for the sake of reference.

In order to ensure the accuracy of the results, three replicates were carried out on fresh samples for each formulation, such that results shown have statistical significance at the 95% confidence level.

Unworked penetration values were determined according to the ASTM D1403 standard, using the Seta universal penetrometer, model 17000–2 (Stanhope-Seta, UK), with a one-quarter cone geometry. The one-quarter-scale penetration values were converted into the equivalent full-scale cone penetration values according to ASTM D217. For the sake of comparison, an approximation of NLGI grade was determined.

Morphological observations of oleogels' microstructure were conducted, at room temperature, with a scanning electron microscope (SEM), model ZEISS EVO LS15 (ZEISS, Germany), at 10 kV. A magnification of 7000 x was used. Previously, all samples were chemically fixed on the holder with 2.5 wt% glutaraldehyde in 0.1 M cacodylate buffer, for 2 h, followed by three washes in 0.1 M cacodylate solution. Subsequently, all samples were subjected to a second fixation with 1 wt% osmium tetraoxide solution, for 1 h, again followed by three washes with 0.1 M cacodylate solution. Finally, all samples were submitted to critical point drying in acetone before being metallized with Au/Pd. Representative morphology prototypes were assured by using, for each formulation studied, at least three different samples and taking five pictures at different locations.

3. Results and discussion

3.1. CNF oleogels' viscous flow behavior

Fig. 1 illustrates the CNF-B oleogels' viscous flow behavior as a function of temperature, at three different concentrations. Thus, the evolution of shear stress with shear rate at selected temperatures between 25 and 180 ºC is displayed for 0.7, 1.4 and 2.8 wt% CNF-B (bleached cellulose nanofibers). Very similar profiles were appreciated with the CNF-U oleogels (not shown).

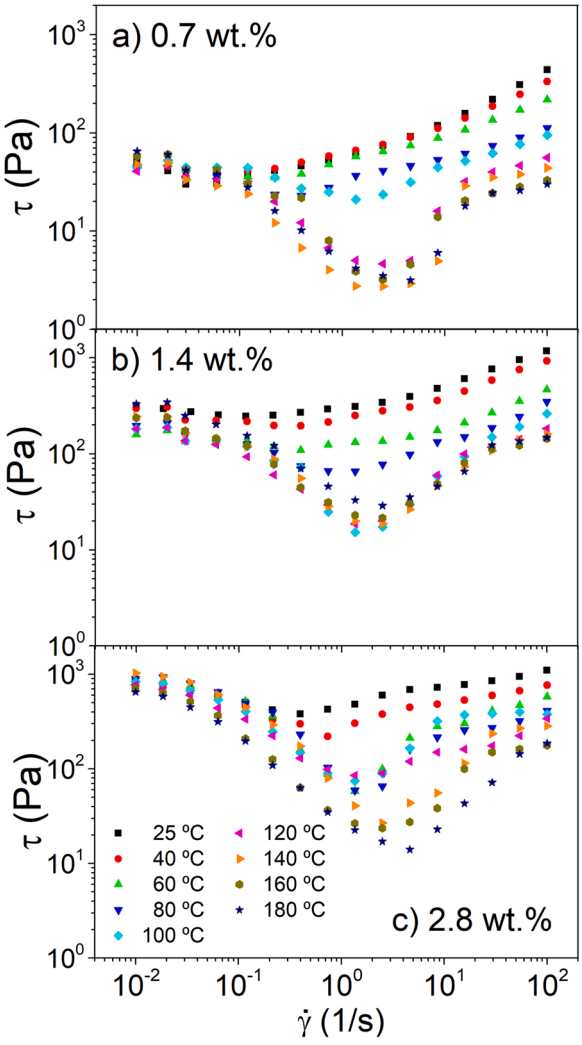

Fig. 1. Evolution of shear stress with shear rate for CNF-B oleogels, at selected temperatures between 25 and 180 ºC, for the three concentrations studied: a) 0.7 wt%; b) 1.4 wt%; c) 2.8 wt%.

Their viscous flow behavior was characterized by a nearly constant value of shear stress at the lowest shear rates. In a similar way to traditional lubricating greases, a minimum value of shear stress had to be applied before the oleogels started flowing, i.e., yielding material [23]. When such a yielding behavior was overcome, a mild increase in the shear stress with the shear rate was observed. This behavior is associated to a reduction in viscosity with increasing the shear rate, i.e., pseudoplastic behavior.

As temperature was raised, a clear minimum in the evolution of the shear stress with shear rate was observed at intermediate shear rate values. As previously pointed out by Britton and Callaghan [24] and Delgado et al. [20,23], such a behavior may correspond to a dynamically non-stable region and may be related to a non-homogeneous field of velocities during the viscometric flow of the oleogels under shear rate sweeps, i.e., the so-called shear banding phenomenon. Therefore, temperature increase seems to have caused disturbances in the oleogels' network which have led to major instabilities in their velocity profile.

The outstanding thickening capacity of nanocellulose in castor oil, which enables gel formation, derives, among other factors, from the existing intermolecular interactions, i.e.,. Van der Waal forces among amphiphilic molecules, mainly intermolecular hydrogen bonding between polar groups. Hydrogen bonds between the hydroxyl groups on a glucose unit of cellulose with other cellulose chains and with the hydroxyl group on the ricinoleic acid of castor oil contribute to the formation of a stable gel-like material. Watanabe et al. [25] reported that weaker H-bonds gradually become dominant with increasing temperature, with the consequent structural changes. Based on the above idea, the higher temperatures would have weakened the existing inter hydrogen bonding within the oleogel's network, which may have caused the unstable viscous flow observed. At 0.7 wt% (Fig. 1a), a very dramatic decay in the shear stress with shear rate was found at 120 ºC, beyond which the flow curves seemed to have reached an asymptotic behavior with temperature. Instabilities were overcome as shear rate was increased beyond 10 s^{-1}, such that the curves suddenly returned to the viscous flow profile observed at lower temperatures. This result suggests that the highest shear rates may induce the free orientation of the cellulose nanofibrils, which normalizes their flow behavior.

As concentration was raised to 1.4 wt% (Fig. 1b), the viscous flow behavior remained essentially the same, but the non-homogeneous flow phenomenon arose at lower temperature and in a more steadily increasing manner. It is worth pointing out that the minimum shear stress value shifted to higher shear rates as temperature was increased. Upon passing the minimum shear stress value, the flow curves evolved following a less pronounced profile than for 0.7 wt%, because a higher concentration of cellulose nanofibrils hampered their free orientation until larger shear rates were imposed. Finally, the 2.8 wt% CNF-B oleogel (Fig. 1c) presented the strongest yielding behavior, in terms of the largest values of shear stress at the lowest shear rates. This result is due to the contribution of a more developed entangled network of nanofibrils. In turn, its viscous flow behavior at intermediate shear rate was found to be unstable even at 25 ºC.

On the other side, Fig. 2 presents a comparative analysis of the effect of the two different types of cellulose nanofibers used on the temperature dependency of the oleogels' viscous flow behavior at the selected concentration of 1.4 wt% nanofiber. Their flow behavior were comparable in terms of the observed minimum in the shear stress versus shear rate curve as temperature was increased. However, noticeable differences can be appreciated as far as their sensitivity to temperature is concerned. In the low to intermediate shear rate window, the 1.4 wt% CNF-U oleogel exhibited lower temperature dependence of its viscous flow behavior as compared to its CNF-B counterpart. Further linear and non-linear viscoelastic measurements may shed light on the issue.

3.2. Thermo-rheological behavior under linear viscoelastic conditions

Fig. 3 shows the evolution of the linear elastic (G') and viscous (G')

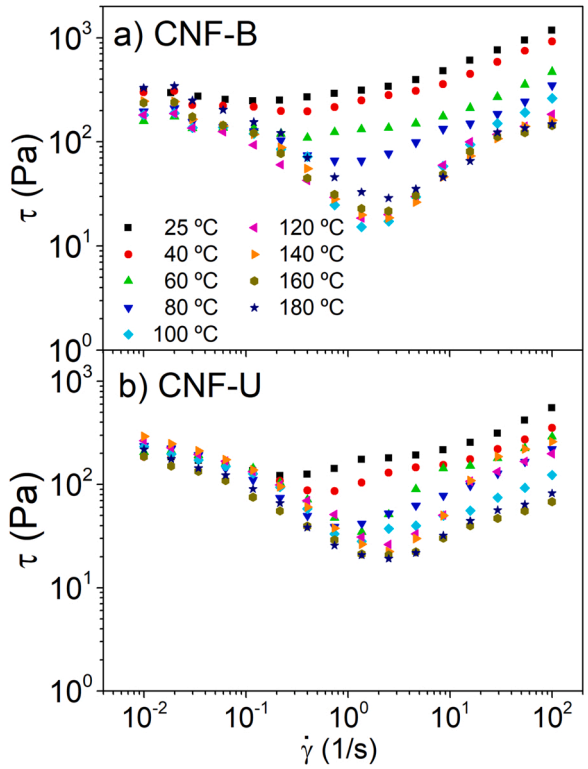

Fig. 2. Evolution of shear stress with shear rate for oleogels with 1.4 wt% cellulose nanofibers, at selected temperatures between 25 and 180 °C, for the two types of nanofibers studied: a) CNF-B; b) CNF-U.

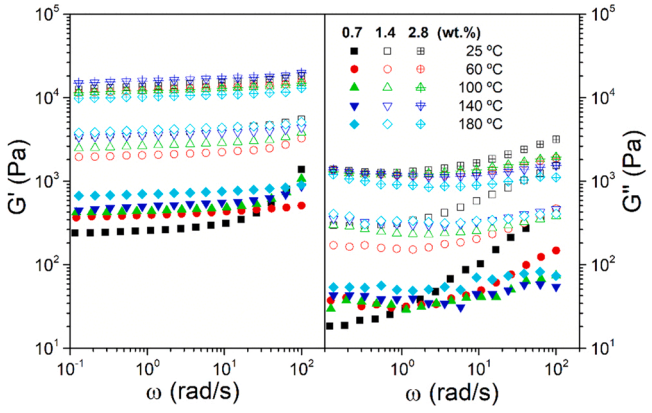

Fig. 3. Evolution of the linear storage (G′) and loss (G″) moduli with frequency for CNF-B oleogels, at selected temperatures between 25 and 180 °C, and for the three concentrations studied.

moduli with frequency, for the CNF-B oleogels, as a function of temperature, in the 25–180 °C interval, and for the three concentrations studied. It is worth highlighting that linear rheology is conducted under very small amplitude oscillatory shear (SAOS) conditions, within the material's linear viscoelastic regime.

As can be appreciated, the G′ curves slightly increased with frequency and remain much higher in comparison with G″ values, i.e., these oleogels exhibit a prevailing elastic behavior. Moreover, the G′′ curves presented a minimum, which resulted to be much less pronounced as temperature was raised. Such a behavior is attributed to the successful formation of cross-linked networks. As later corroborated through SEM imaging, the dynamic mechanical spectra shown in Fig. 3 denotes the existence of topological restrains as a consequence of physical cross-linking. Hence, the olegels exhibited intermediate properties between those of an entanglement network (pseudogel) and a physical gel, according to the characteristics reported by Ross-Murphy [26] for these types of materials. Such a behavior closely resembles the rheological response of conventional lubricating greases [27].

An increase in nanofiber concentration brought about noticeable quantitative differences. Both linear viscoelastic moduli remarkably increased with concentration (almost two decades between 0.7 and 2.8 wt%), due to an increase in the cross-links density with the oleogels' structural skeleton. This result is in accordance with the reduction in their penetration values, as commented above. Thus, varying CNF (thickener) concentrations within the narrow interval studied enabled to modulate the grease consistency for lubricant applications, thereby denoting the extraordinary thickening power of these cellulose nanofibers. In addition, it was observed that G′ is substantially higher than G″ within the full temperature range studied, suggesting that the gelled state can be maintained even at 180 °C. Even though their qualitative behavior did not vary too much, larger nanofiber concentrations resulted in a reduced thermal dependence of the linear viscoelastic functions. Under small amplitude oscillatory deformations, the enhanced elasticity resulting from a denser network seemed to be much less affected by temperature.

Surprisingly, an unexpected increase of the elastic modulus with temperature was observed at the low and intermediate concentrations, i.e., 0.7 and 1.4 wt%. In a lubricating grease the thickener acts as a "sponge" which retains the base oil. It might be that if the thickener network is not sufficiently dense (0.7 and 1.4 wt%) and the oil viscosity is remarkably reduced with increasing temperature, it may leak the oil. As a consequence, the oleogel's effective concentration would increase, thereby yielding higher elasticity. When the nanofiber concentration was increased up to 2.8 wt%, a more suitable behavior was found, given that the thickener was able to retain the base oil even at the highest temperatures studied.

It is noteworthy that the storage modulus values for the 2.8 wt% CNF-B oleogel are quite similar to those shown by traditional lubricating greases with NLGI grade 2 or 3, which are typically located between 10^4 and 10^5 Pa, and are around one order of magnitude higher than their corresponding loss modulus values [23,27]. Even so, the observed temperature-dependence was very different to that described for traditional lithium greases. For a model lubricating grease containing 14 wt % lithium 12-hydroxystearate, Delgado et al. [20] reported a dramatic change in the slope of the so-called plateau modulus, G^0_N, versus temperature at a critical temperature of around 110 °C. G^0_N, defined as the G′ value at the frequency where the minimum in G′′ appears, is a measure of both the entanglement degree and the strength of the gel-like structure. This result, therefore, demonstrates a dramatic loss of consistency of such a lithium grease upon 110 °C, which can be related with its maximum operating temperature, usually denoted as dropping point [20]. Those authors reported noticeable changes in the microstructure network of the lithium grease due to thermal effects. Contrarily, the behavior of the oleogels herein studied was such that G^0_N remained quite stable with temperature, above all the formulation with the largest nanofiber concentration, i.e., 2.8 wt%.

Furthermore, Fig. 4 illustrates the influence of nanofiber type, at a concentration of 1.4 wt%, on the frequency-dependence of G′ and G′′ over the same previously studied temperature range between 25 and 180 °C. In general, the effect of temperature on the linear viscoelastic functions was less pronounced than in the previously reported viscous flow behavior. It followed the evolution of the yield stress with temperature observed in Fig. 2 at the low shear rate region on the viscous flow curve, where linear viscoelastic conditions still remain. The short range motion typical from the LVE region is much less constrained by the existing physical interactions than the large deformations involved in a viscous flow test. In the low frequency range, both CNF-B and CNF-U presented quite comparable sensitivity to temperature.

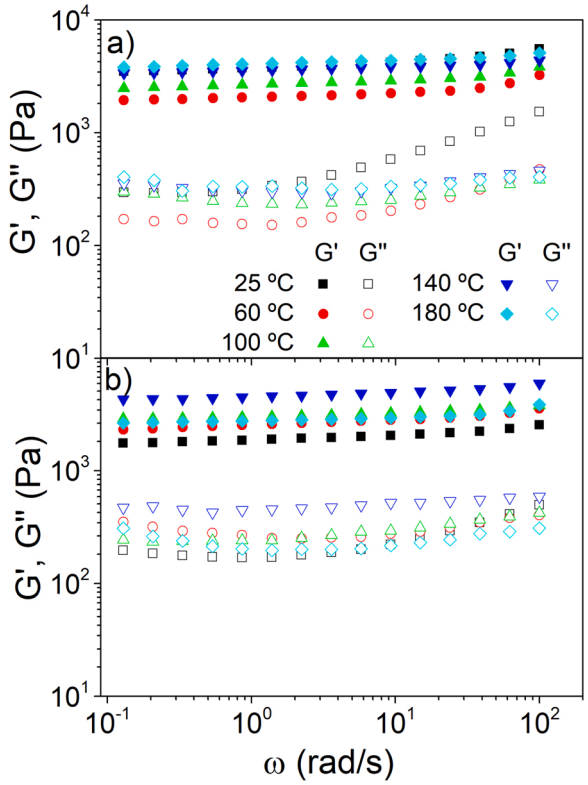

Fig. 4. Evolution of the linear storage (G) and loss (G) moduli with frequency for oleogels containing 1.4 wt% nanocellulose, at selected temperatures between 25 and 180 °C, for the two nanofibers studied: a) CNF-B; b) CNF-U.

3.3. CNF oleogels' response to "rheo-destruction" and "rheo-recovery" tests

Further the above discussion on the thermo-rheological characterization within the linear viscoelastic regime, the non-linear viscoelastic behavior of the oleogels was analyzed through tests which quantified the materials' response to the application of an external stress beyond the LVE region. The application of non-linear shear stresses may result in the disturbance of the grease's mechanical stability. Hence, its analysis may help to assess the functional properties of these oleogels [20]. Moreover, the extent of the oleogels' ulterior recovery back to their initial unaltered state was also assessed (see Section 2.3 for details). The results were plotted as the evolution of the complex shear modulus |G* |, at a selected frequency of 6.28 rad/s (1 Hz), versus the elapsed time, in log-linear plots.

Fig. 5 illustrates the results of dynamic time sweep tests, at 25 °C, for the three CNF-B oleogels studied (0.7, 1.4 and 2.8 wt%) as a function of the stress imposed. Over the first 5 min a stress within the LVE regime was applied such that the material stiffness was evaluated with no alteration of its intrinsic microstructure. Obviously, constant values of | G* | were obtained for each set of experiments. Subsequently, the stress imposed was increased up to the corresponding non-linear target values and maintained during the following 30 min. An instant decay in |G* | related to structural network alterations was observed. Table 2 displays the percentage of "rheo-destruction", defined as the ratio of the observed decay in the complex modulus, $|G_0^*| - |G_1^*|$, relative to the sample unaltered state, $|G_0^*|$. In all cases, little destruction was observed at 20 Pa, the limit of the LVE regime (results not included in Table 2). Outside the LVE regime, very noticeable percentages of destruction, which increased with the stress value, were observed at the lowest concentration. Hence, values of 89.1% and 91.5% were found at 100 and 200 Pa, respectively, for the 0.7 wt% CNF-B oleogel. However, as the concentration was raised, the damage done to the oleogels was

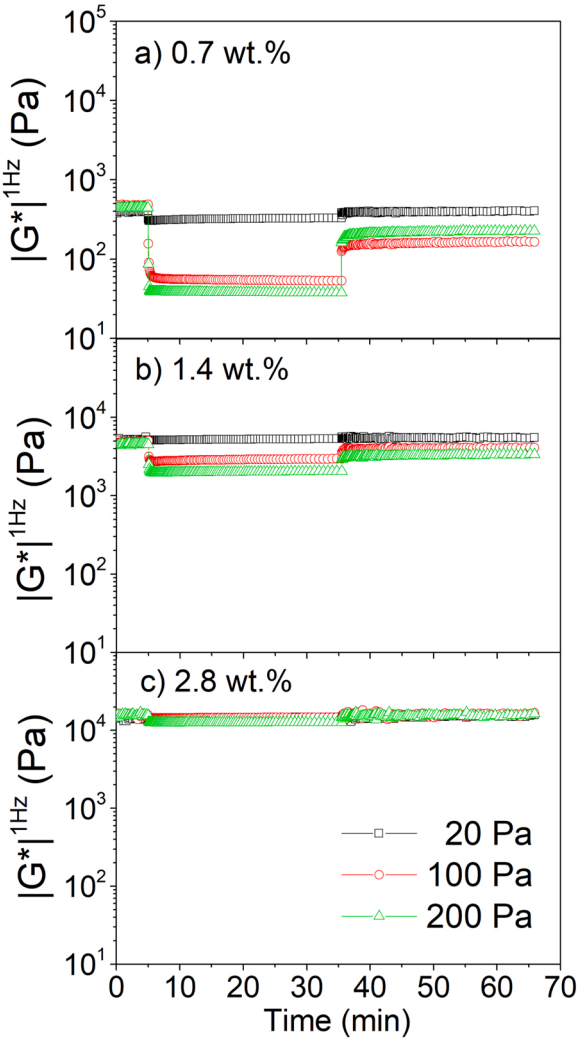

Fig. 5. Time evolution of the dynamic shear modulus, |G* |, at 1 Hz and 25 °C, for CNF-B oleogels, at selected non-linear shear stresses, for the three concentrations studied: a) 0.7 wt%; b) 1.4 wt%; c) 2.8 wt%.

remarkably reduced. In fact, the 2.8 wt% CNF-B oleogel seemed to remain almost unaffected even at 200 Pa (results not included in Table 2). Hence, the addition of higher concentrations of nanofibrils was found to shift the oleogel's LVE threshold to remarkably larger stress values. This fact underscores the key role of the cellulose nanofibrils to develop lubricating ecogreases with enhanced elasticity and improved mechanical stability.

Moreover, an instant partial recovery of the complex modulus values was observed after the material was returned to the LVE regime (the same shear stress as applied in the initial stage). Table 2 also displays the percentage of "rheo-recovery", defined as the ratio of the observed recovery in the complex modulus of the altered sample, $|G_2^*| - |G_1^*|$, relative to the previous imparted destruction, $|G_0^*| - |G_1^*|$. Thus, the lower the %-recovery is, the higher the degree of irreversible structural alteration as a consequence of the sample's LVE limit being exceeded. As shown in Table 2, the 0.7 wt% CNF-B oleogel presented lower values of %-recovery than the 1.4 wt% oleogel, which is consistent with the much larger %-destruction. Even so, it is noteworthy that the %-recovery found at 200 Pa for the 0.7 wt% CNF-B oleogel, 46.4%, was higher than at 100 Pa, 25.5%. The 0.7 wt% CNF-U oleogel results (not shown) led to the same conclusion. It seems that 200 Pa provoked a more severe disruption to the nanofibers network, which would have rearranged in a more favorable disposition when the material returned to its LVE regime [28]. This situation did not occur at higher nanofiber concentration

because the network was probably too dense so as to enable further rearrangements.

In a similar way, Fig. 6 shows the results corresponding to the two types of nanofibers, CNF-B and CNF-U, at a constant 1.4 wt% concentration. Remarkable differences were observed between them, since the CNF-B oleogel ruptures and fails, while the CNF-U oleogel withstands the large shear deformations more efficiently and recovers its previous state in a larger extent. As can be observed in Fig. 6b and Table 2, the CNF-U oleogel presented much lower values of %-destruction (13.3% at 100 Pa) and largest values of %-recovery (100% at 100 Pa). In turn, larger %-destruction and smaller %-recovery were found both at 100 and 200 Pa for the CNF-B oleogel (Fig. 6a and Table 2). It was thereby confirmed that under LAOS (large amplitude oscillatory shear) conditions, both oleogels presented noticeable different behaviors. Therefore, the CNF-B oleogel seemed to behave as a stronger physical gel, i.e., with a stiffer structure from a rheological perspective, and the CNF-U oleogel seemed to behave as a weaker physical gel according to the characteristics reported by Ross-Murphy [26]. It is worth pointing out that the CNF-U oleogel showed a similar mechanical behavior to the model lubricating grease containing 14 wt% lithium 12-hydroxystearate studied by Delgado et al. [20]. As previously reported by Iglesias et al. [18] and Lê et al. [29], residual lignin significantly affects the rheological properties of cellulose nanofibril suspensions. Thus, the CNF-U oleogel proved to be, from a mechanical standpoint, more resistant than the CNF-B oleogel, due to the existing interactions between fibrils-lignin and lignin-lignin.

3.4. *Analysis of the CNF oleogels' thermo-rheological behavior based on chemical and microstructural considerations*

The bleaching process seems to have had a remarkable impact on the way that CNF-B nanofibers arranged such that its final oleogel showed much higher sensitivity to temperature and loading time under large shear deformations.

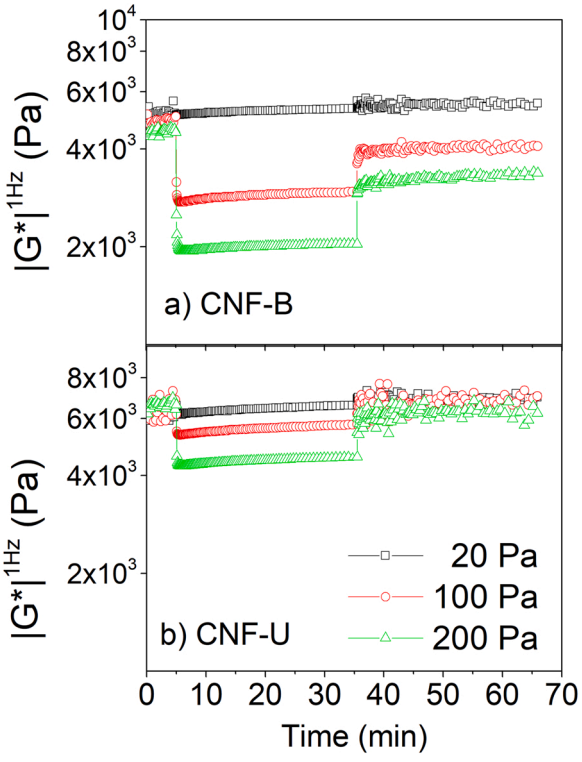

Fig. 6. Time evolution of the dynamic shear modulus, |G* |, at 1 Hz and 25 ºC, for 1.4 wt% nanocellulose oleogels, at selected non-linear shear stresses, for the two nanofiber types studied: a) CNF-B; b) CNF-U.

With regard to the nanofibers chemical composition, Table 1 demonstrates that bleaching caused some minor differences in terms of the celluloses (glucan) and hemicelluloses (xylan) content as compared to the unbleached nanofibers. Moreover, their glucuronic acid content remained essentially the same, given that the bleaching process mainly attacks (removes and oxidates) the lignin, not the cellulose fraction. Obviously, CNF-B had lower lignin content (1.7 wt%) than CNF-U (2.6 wt%). Therefore, from the nanofibers chemical composition point of view, the lignin content may affect the observed thermo-rheological differences between the oleogels studied. In fact, Lê et al. [29] pointed out that the presence of lignin influences the level of aggregation and elasticity within the nanocellulose gel-network.

In addition, as far as pulp mechanical pretreatment is concerned, a lower lignin content seems to favor defibrillation [18,30]. As de Souza Fonseca et al. [30] remarked, this condition facilitates swelling of the fibers and improves deconstruction of the fiber cell wall. Consequently, the bleaching process yielded an improved nanofibrillation performance of 60.8% nano-sized fibrils, as compared to CNF-U with 50.2% nano-sized fibrils (Table 1). It is worth to pointing out that it might be the reason behind the so large difference in nanofibrils' length. Thus, the bleaching treatment seems to improve the fiber exfoliation from the elm pulp, yielding longer nanofibers in the nanofibril suspension. This better nanofibrillation yield of CNF-B was also justified by its higher ζ-potential value in the starting hydrogel, as it was suggested by Jiménez-López et al. [22].

The Scanning Electron Microscopy (SEM) micrographs, shown in Fig. 7, may help clarify the issue. Figs. 7a and 7b for CNF-B and CNF-U, respectively, display similar entangled networks of cellulose nanofibers, but also of non-nanofibrillated microfibrils.However, the size of cavities among cellulose nanofibers where oil is trapped were smaller for CNF-U-based entangled network, which suggests a larger level of aggregation of the nanofibers gel-network [29]. Such a structural rearrangement of CNF-U nanofibers involved a better mechanical resistance to large amplitude oscillatory shear conditions than in the CNF-B-based oleogels (Fig. 6).

Based on such an information, and given that both CNF-B and CNF-U oleogels are constituted by physical crosslinking and inter-chain hydrogen bonding, the following explanation is provided. The hydrogen bonding might be playing the role of semi-permanent junction points among the cellulose nanofibers. The CNF-U oleogel, with shorter and lower percentage of nanofibers, may still relax and accommodate to the application of large deformations. In turn, the relaxing process in the CNF-B oleogel might be constrained by the existence of more junction points due to the existence of much longer chain Table 2.

4. Conclusions

Cellulose nanofiber-based oleogels containing nanofibers which derived from bleached and unbleached pulps were successfully prepared. In both cases, relatively compact fibrous microstructures of entangled nanofibers, but also of non-nanofibrillated microfibrils, were achieved. Significant differences, in terms of their thermo-rheological

Table 1
Chemical composition, nanofibrillation yield, ζ-potential and dimensions of the two types of cellulose nanofibrils studied [22].

Chemical composition				
Type	Glucan (wt%)	Xylan (wt%)	Glucuronic ac. (wt%)	Total lignin (wt%)
CNF-B	82.6 ± 0.1	14.7 ± 0.1	1.0 ± 0.2	1.7 ± 0.3
CNF-U	80.0 ± 0.6	16.4 ± 0.1	1.1 ± 0.1	2.6 ± 0.2
Physico-chemical properties				
Type	**Nanofibrillation yield (%)**	**ζ-potential (mV)**	**D (nm)**	**L (nm)**
CNF-B	60.8 ± 2.5	-28.4	5.9 ± 1.7	1237 ± 680
CNF-U	50.2 ± 2.4	-7.4	3.7 ± 0.7	370 ± 14

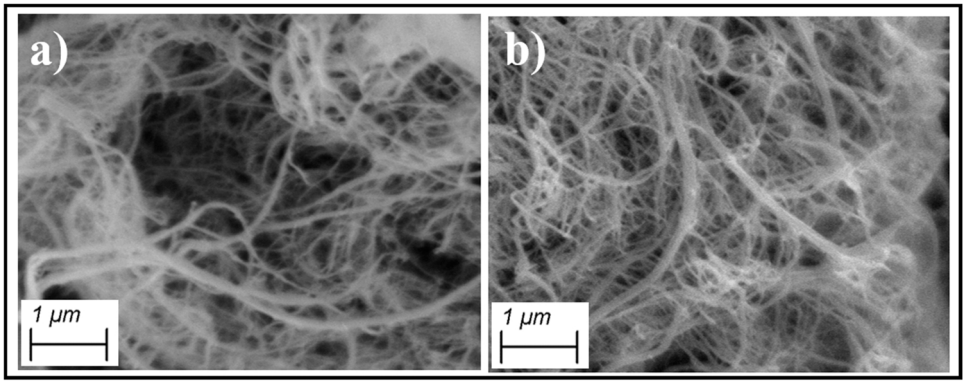

Fig. 7. SEM micrographs corresponding to 1.4 wt% nanocellulose oleogels, for the two types of nanofibers studied: a) CNF-B; b) CNF-U.

Table 2
Rheological destruction and recovery percentages of the oleogels studied, after the application of different shear stresses outside the linear viscoelasticity region, as a function of type and concentration of cellulose nanofibrils.

Oleogels	CNF content (wt%)	Non-linear stress value (Pa)	%-destruction	%-recovery
CNF-B	0.7	100	89.1	25.5
		200	91.5	46.4
	1.4	100	41.4	54.1
		200	55.7	52.0
CNF-U	1.4	100	13.3	100
		200	28.9	90.3

behavior, were observed. It was concluded that a lower lignin content seems to be effective on the defibrillation process, thereby yielding an improved nanofibrillation performance and larger nanofibers for CNF-B. In this sense, the CNF-B oleogel showed evidences of being a stronger physical gel, i.e., with a stiffer structure from a rheological perspective, than the CNF-U oleogel. Moreover, the hydrogen bonding among nanofibers might be playing the role of semi-permanent junction points, in such a way that the oleogel with shorter and lower percentage of nanofibers, i.e., CNF-U oleogel, may relax and accommodate to the application of large deformations. On the contrary, the relaxation process in the CNF-B oleogel, involving much longer nanofibers, would be hindered by the existence of more junction points. Unbleached cellulose nanofibers were, thereby, found to perform better than their bleached counterparts from a thermo-rheological perspective. In addition, the CNF-B oleogel was more sensitive to temperature than the CNF-U oleogel.

CRediT authorship contribution statement

Conceptualization, M.A.D., M.G.-M. and C.R.; Methodology, C.R. and S.D.F.-S.; Software, C.R. and S.D.F.-S.; Validation, M.A.D. and M.G.-M.; Formal analysis, M.A.D. and M.G.-M.; Investigation, C.R., S.D.F.-S., M.A.D. and M.G.-M.; Resources, S.D.F.-S. and M.A.; Data curation, C.R. M.A.D. and M.G.-M.; Writing—original draft preparation, C.R. and M.G.-M.; Writing—review and editing, M.G.-M. and M.A.D.; Visualization, M.A.D., M.G.-M. and C.R.; Supervision, M.A.D. and M.G.-M.; Project administration, M.A.D. and M.G.-M.; Funding acquisition, M.A.D. and M.G.-M. All authors have read and agreed to the published version of the manuscript.

Declaration of Competing Interest

The authors declare that they have no known competing financial interests or personal relationships that could have appeared to influence the work reported in this paper.

Data availability

Data will be made available on request.

Acknowledgements

This work is part of two Research Projects sponsored by “Programa Operativo FEDER-Andalucía 2014–2020″ (UHU-1255843 and UHU-202008). Funding for open access charge: Universidad de Huelva/CBUA. The authors gratefully acknowledge their financial support. S.D. Fernández-Silva acknowledges “Ayudas para la Contratación Predoctoral de Personal Investigador en Formación 2021, Junta de Andalucía” (PREDOC_01696), for funding his PhD Thesis.

References

[1] J.A. Cecilia, D. Ballesteros, R.M. Alves, F. Murilo, C.L. Cavalcante Jr., E. Rodríguez-Castellón, An overview of the biolubricant production process: challenges and future perspectives, Processes 8 (2020) 257, https://doi.org/10.3390/pr8030257.
[2] T.M. Panchal, A. Patel, D.D. Chauhan, M. Thomas, J.V. Patel, A methodological review on bio-lubricants from vegetable oil based resources, Renew. Sustain. Energy Rev. 70 (2017) 65–70, https://doi.org/10.1016/j.rser.2016.11.105.
[3] R. Narayana Sarma, R. Vinu, Current status and future prospects of biolubricants: properties and applications, Lubricants 2022 (10) (2022) 70, https://doi.org/10.3390/lubricants10040070.
[4] L.A. Quinchia, M.A. Delgado, T. Reddyhoff, C. Gallegos, H.A. Spikes, Tribological studies of potential vegetable oil-based lubricants containing environmentally friendly viscosity modifiers, Tribology Int. 69 (2014) 110–117, https://doi.org/10.1016/j.triboint.2013.08.016.
[5] M.A. Delgado, L.A. Quinchia, H.A. Spikes, C. Gallegos, Suitability of ethyl cellulose as multifunctional additive for blends of vegetable oil-based lubricants, J. Clean. Prod. 151 (2017) 1–9, https://doi.org/10.1016/j.jclepro.2017.03.023.
[6] S.D. Fernández-Silva, M.A. Delgado, M.V. Ruiz-Méndez, I. Giráldez, M. García-Morales, Potential valorization of waste cooking oils into sustainable bio-lubricants, Ind. Crops Prod. 185 (2022), 115109, https://doi.org/10.1016/j.indcrop.2022.115109.
[7] R. Sánchez, J.M. Franco, M.A. Delgado, C. Valencia, C. Gallegos, Thermal and mechanical characterization of cellulosic derivatives-based oleogels potentially applicable as bio-lubricating greases: influence of ethyl cellulose molecular weight, Carbohydr. Polym. 83 (2011) 151–158, https://doi.org/10.1016/j.carbpol.2010.07.033.
[8] G. Domínguez, A. Blánquez, A.M. Borrero-López, C. Valencia, M.E. Eugenio, M. E. Arias, J. Rodríguez, M. Hernández, Eco-friendly oleogels from functionalized kraft lignin with laccase SilA from streptomyces ipomoeae: an opportunity to replace commercial lubricants, ACS Sustain. Chem. Eng. 9 (2021) 4611–4616, https://doi.org/10.1021/acssuschemeng.1c00113.
[9] A.H. Tayeb, E. Amini, S. Ghasemi, M. Tajvidi, Cellulose nanomaterials-binding properties and applications: a review, Molecules 23 (2018) 2684, https://doi.org/10.3390/molecules23102684.
[10] P.G. Marakana, A. Dey, B. Saini, Isolation of nanocellulose from lignocellulosic biomass: synthesis, characterization, modification, and potential applications, J. Environ. Chem. Eng. 9 (2021), 106606, https://doi.org/10.1016/j.jece.2021.106606.
[11] E.J. Foster, R.J. Moon, U.P. Agarwal, M.J. Bortner, J. Bras, S. Camarero-Espinosa, K.J. Chan, M.J.D. Clift, E.D. Cranston, S.J. Eichhorn, D.M. Fox, W.Y. Hamad, L. Heux, B. Jean, M. Korey, W. Nieh, K.J. Ong, M.S. Reid, S. Renneckar, R. Roberts, J.A. Shatkin, J. Simonsen, K. Stinson-Bagby, N. Wanasekara, J. Youngblood, Current characterization methods for cellulose nanomaterials, Chem. Soc. Rev. 8 (2018) 1–71, https://doi.org/10.1039/C6CS00895J.

[12] Q. Ding, J. Zeng, B. Wang, D. Tang, K. Chen, W. Gao, Effect of nanocellulose fiber hornification on water fraction characteristics and hydroxyl accessibility during dehydration, Carbohydr. Polym. 207 (2018) 44–51, https://doi.org/10.1016/j.carbpol.2018.11.075.
[13] T. Li, C. Chen, A.H. Brozena, J.Y. Zhu, L. Xu, C. Driemeier, J. Dai, O.J. Rojas, A. Isogai, L. Wagberg, L. Hu, Developing fibrillated cellulose as a sustainable technological material, Nature 590 (2021) 47–56, https://doi.org/10.1038/s41586-020-03167-7.
[14] C. Roman, M. García-Morales, M.E. Eugenio, D. Ibarra, R. Martín-Sampedro, M. A. Delgado, A sustainable methanol-based solvent exchange method to produce nanocellulose-based ecofriendly lubricants, J. Clean. Prod. 319 (2021), 128673, https://doi.org/10.1016/j.jclepro.2021.128673.
[15] O. Nechyporchuk, M.N. Belgacem, J. Bras, Production of cellulose nanofibrils: a review of recent advances, Ind. Crops Prod. 93 (2016) 2–25, https://doi.org/10.1016/j.indcrop.2016.02.016.
[16] H.-J. Kim, S. Roy, J.-W. Rhim, Effects of various types of cellulose nanofibers on the physical properties of the CNF-based films, J. Environ. Chem. Eng. 9 (2021), 106043, https://doi.org/10.1021/acsami.1c06204.
[17] M. Rajinipriya, M. Nagalakshmaiah, M. Robert, S. Elkou, Importance of agricultural and industrial waste in the field of nanocellulose and recent industrial developments of wood based nanocellulose: a review, ACS Sustain. Chem. Eng. 6 (2018) 2807–2828, https://doi.org/10.1021/acssuschemeng.7b03437.
[18] M.C. Iglesias, N. Shivyari, A. Norris, R. Martín-Sampedro, M.E. Eugenio, P. Lahtinen, M.L. Auad, T. Elder, Z. Jiang, C.E. Frazier, M.S. Peresin, The effect of residual lignin on the rheological properties of cellulose nanofibril suspensions, J. Wood Chem. Technol. 40 (2020) 370–381, https://doi.org/10.1080/02773813.2020.1828472.
[19] M. Jonoobi, Jalaludin Harun, A. Shakeri, M. Misra, K. Oksman, A chemical composition, crystallinity, and thermal degradation of bleached and unbleached Kenaf bast (Hibiscus cannabinus) pulp and nanofibers, Bioresources 4 (2009) 626–639, https://doi.org/10.15376/BIORES.4.2.626-639.
[20] M.A. Delgado, C. Valencia, M.C. Sánchez, J.M. Franco, C. Gallegos, Thermorheological behaviour of a lithium lubricating grease, Tribology Lett. 23 (2006) 47–54, https://doi.org/10.1007/s11249-006-9109-5.
[21] D.S. Ogunniyi, Castor oil: a vital industrial raw material, Bioresour. Technol. 97 (2006) 1086–1091, https://doi.org/10.1016/j.biortech.2005.03.028.
[22] L. Jiménez-López, M.E. Eugenio, D. Ibarra, M. Darder, J.A. Martín, R. Martín-Sampedro, Cellulose nanofibers from a dutch elm disease-resistant ulmus minor clone, Polymers 12 (2020) 2450, https://doi.org/10.3390/polym12112450.
[23] M.A. Delgado, S. Secouard, C. Valencia, J.M. Franco, On the steady-state flow and yielding behaviour of lubricating greases, Fluids 4 (2019) 6, https://doi.org/10.3390/FLUIDS4010006.
[24] M.M. Britton, P.T. Callaghan, NMR visualisation of anomalous flow in cone-and-plate rheometry, J. Rheol. 41 (1997) 1365–1386, https://doi.org/10.1122/1.550846.
[25] A. Watanabe, S. Morita, Y. Ozaki, Temperature-dependent structural changes in hydrogen bonds in microcrystalline cellulose studied by infrared and near-infrared spectroscopy with perturbation-correlation moving-window two-dimensional correlation analysis, Appl. Spectrosc. 60 (2006) 611–618, https://doi.org/10.1366/000370206777670549.
[26] S.B. Ross-Murphy, Structure-property relationships in food biopolymer gels and solutions, J. Rheol. 39 (1995) 1451, https://doi.org/10.1122/1.550610.
[27] R. Sánchez, C. Valencia, J.M. Franco, Rheological and tribological characterization of a new acylated chitosan–Based biodegradable lubricating grease: a comparative study with traditional lithium and calcium greases, Tribology Trans. 57 (2014) 445–454, https://doi.org/10.1080/10402004.2014.880541.
[28] C. Roman, M.A. Delgado, M. García-Morales, Fatigue performance evaluation of bitumen mastics reinforced with polyolefins through a dissipated energy approach, Mater. De. Constr. 70 (338) (2020), e217, https://doi.org/10.3989/mc.2020.09319.
[29] H.Q. Lê, K. Dimic-Misic, L.S. Johansson, T. Maloney, H. Sixta, Effect of lignin on the morphology and rheological properties of nanofibrillated cellulose produced from γ-valerolactone/water fractionation process, Cellulose 25 (2018) 179–194, https://doi.org/10.1007/s10570-017-1602-5.
[30] A. De Souza Fonseca, S. Panthapulakkal, S. Kumar Konar, M. Sain, L. Bufalinof, J. Raabe, I.P. De Andrade Miranda, M.A. Martins, G.H. Denzin Tonoli, Improving cellulose nanofibrillation of non-wood fiber using alkaline and bleaching pre-treatments, Ind. Crops Prod. 131 (2019) 203–212, https://doi.org/10.1016/j.indcrop.2019.01.046.